Entropic algorithms and the lid method as exploration tools for complex landscapes

Daniele Barettin[1] and Paolo Sibani[2,*]

[1]*Mads Clausen Institute for Product Innovation, University of Southern Denmark, DK-6400 Sønderborg, Denmark*

[2]*Institut for Fysik og Kemi, SDU, DK-5230 Odense M, Denmark*

(Received 12 April 2011; revised manuscript received 18 July 2011; published 16 September 2011)

Monte Carlo algorithms such as the Wang-Landau algorithm and similar "entropic" methods are able to accurately sample the density of states of model systems and thereby give access to thermal equilibrium properties at any temperature. Thermal equilibrium is, however, unachievable at low temperatures in glassy systems. Such systems are characterized by a multitude of metastable configurations pictorially referred to as "valleys" of an energy landscape. Geometrical properties of the landscape, e.g., the local density of states describing the distribution in energy of the states belonging to a single valley, are key to understanding the dynamical properties of such systems. In this paper we combine the lid algorithm, a tool for landscape exploration previously applied to a range of models, with the Wang-Swendsen algorithm. To test this improved exploration tool, we consider a paradigmatic complex system, the Edwards-Anderson model in two and three spatial dimensions. We find a striking difference between the energy dependence of the local density of states in two dimensions and three dimensions—nearly linear in the first case, and nearly exponential in the second. The dynamical consequences of these findings are discussed.

DOI: 10.1103/PhysRevE.84.036706 PACS number(s): 05.10.−a, 65.60.+a, 61.43.Fs

I. INTRODUCTION

Energy landscapes of model systems have been studied extensively using a variety of numerical methods specialized for different purposes [1]. For example, using repeated thermal quenches, each quench leading to the local energy minimum configuration or inherent state [2] which lies below the current state of a Monte Carlo (MC) simulation, the landscape is partitioned into the catchment basins belonging to the different inherent states. Identifying the important connections between these basins, i.e., typically, the "mountain passes" of lowest energy, one can then produce a coarse-grained version of the landscape and use it to assess both dynamical and equilibrium properties. This approach encounters problems in models of glassy systems, which feature a quasicontinuum of metastable configurations, each configuration parameterized by an energy barrier gauging its thermal stability and its lifetime under isothermal conditions.

If equilibrium thermal properties are of interest, entropic or "flat histogram" methods [3–5] are powerful and generally applicable tools. These methods avoid the trapping in local energy minima which plagues the standard Metropolis algorithm and produce the global density of states (GDOS) as a function of the energy. From there, any thermal equilibrium property of interest can be obtained. Since, however, thermal equilibrium is not experimentally achievable in glassy systems at low temperatures, equilibrium properties of pertinent models have mainly academic interest.

Local geometrical features of the energy landscape as extracted by the lid method have a direct bearing on the dynamical properties of glassy model systems: a fictitious and impenetrable energy barrier, called a "lid," is introduced and the energy distribution of all the microstates which can be reached starting from a given inherent state without ever crossing the lid energy is determined. The distribution is called local density of states (LDOS) and gives access to the local equilibrium properties of the (fictitious) valley jointly defined by an inherent state and a lid, just like the density of states provides corresponding global information. Furthermore, the thermal stability of a valley at a given temperature is encoded in the LDOS.

Finding the LDOS can be numerically challenging. Metropolis sampling at low temperatures is hampered by the large number of local minima, while at high temperature, trajectories linger in many cases just below the lid energy due to the great number of states available there. In both cases the result is poor sampling. Exhaustive enumeration was utilized in Refs. [6–10] to avoid these problems. That procedure is both fast and exact but puts very high demands on memory availability and quickly runs out of space when the system size and/or the energy range is large.

In this paper we show how the LDOS can be efficiently estimated by combining the lid method with the flat histogram method of Wang and Landau [4]. From an algorithmic point of view, imposing a lid restricts the search space. While this hardly changes the overall convergence properties of the histogram method, the lid makes it possible to obtain a far more accurate description of the density of states in the low-energy region close to the ground state of the model investigated. As shown below, this accuracy is not guaranteed by the unrestricted entropic method, since the tiny fraction of all the available configurations present near the ground state can be extremely hard to sample. Compared to the lid method in combination with an exhaustive search, the present approach is far more powerful—larger systems can be investigated over a much larger range of energies.

In this paper the algorithm is applied to the Edwards-Anderson (EA) [11] spin-glass model, a paradigmatic glassy system featuring quenched disordered interactions. We find that the energy dependencies of the LDOS in two dimensions (2D) and three dimensions (3D) differ considerably, and that the 3D results concur with important experimental features of real spin glasses.

*paolo.sibani@ifk.sdu.dk

II. METHOD AND MODEL

Since key properties of experimental spin glasses [11] are reproduced by Monte Carlo simulations of the EA model, the latter can be considered a bona fide complex system in its own right [12,13]. For completeness, we briefly describe the model and the relevant features of its energy landscape before turning to how entropic sampling and the lid method are jointly applied to the EA model.

A. The Edwards-Anderson model and the lid method

In the EA model Ising spins, $S_i = \pm 1$, are placed on a cubic lattice and interact with their nearest neighbors through quenched random couplings. A system of N Ising spin in configuration x has an energy $E(x)$ given by

$$E(x) = -\frac{1}{2}\sum_{ij} J_{ij} S_i^x S_j^x - H\sum_i S_i^x, \tag{1}$$

where the coupling matrix $\mathbf{J}$ is symmetric, with elements J_{ij} vanishing unless the sites i and j are neighbors on the lattice. For $i < j$, the nonzero couplings are random independent variables, drawn in our case from a Gaussian distribution, with zero average and unit variance. The last term in Eq. (1) describes the interaction with an external magnetic field H.

In 3D, at $H = 0$ and for temperatures below a critical temperature $T_c \approx 0.95$ (see Ref. [14] for a chronologically ordered list of different T_c estimates) the model is in its spin-glass phase, which is characterized by a nonzero value of the spin-glass order parameter [15,16].

At low energies the energy landscape of the EA model features a multitude of nested metastable "valleys," i.e., regions of configuration space which support a metastable equilibriumlike probability distribution [7]. A valley jointly defined by an inherent state of energy $E_{\min}$ and a lid energy $E_{\text{lid}} > E_{\min}$ comprises all configurations connected to the inherent states by paths (i.e., series of single spin flips) never crossing the lid energy. For each valley exhaustive enumeration of all states below the lid is implemented up to the lid value which opens a connection to a new inherent state of lower energy [7]. For rather small systems, the LDOS thus obtained seems to grow in a near exponential fashion (see also [17]). The lid dependence of the rate of growth has not been clarified, nor is it clear how the property extends to larger systems.

B. The entropic sampling algorithm

Entropic sampling is a Monte Carlo technique invented by Lee [5] where transitions are controlled by (the current estimate of) the density of states $\varrho(E)$. Rather than sampling with the usual Boltzmann weight $e^{-(E/T)}$, the entropic method samples with a probability $\propto \frac{1}{\varrho(E)}$. Unlike the energy, the density of states ϱ is not known beforehand and must hence be calculated iteratively during the simulation. Starting with a (poor) guess $\varrho_1(E) =$ constant, we divide the energy axis into a certain number of bins, calculate a histogram $h_1(E)$ of the energies of the states visited, and normalize it to one. The probability $h_1(E)$ to visit an energy bin E is proportional to the number of states $\varrho_1(E)$ multiplied by the probability $1/\varrho_1(E)$ with which we sampled, i.e.,

$$\varrho(E) \propto \varrho_1(E) h_1(E). \tag{2}$$

We use the above to iteratively define

$$\varrho_{n+1}(E) = \varrho_n(E) h_n(E), \tag{3}$$

which specifies the algorithm in terms of successive approximations to the density of states. In terms of the microcanonical entropy

$$S(E) = \log \varrho(E), \tag{4}$$

the algorithm reads

$$S_{n+1}(E) = S_n(E) + \log h_n(E), \tag{5}$$

from which is clear that the probability of sampling a particular state is proportional to $e^{-S(E)}$, and that convergence implies $h_n(E) \to 1$ for $n \to \infty$. For a general discussion of entropic algorithms, we refer the reader to the book by Newman and Barkema [18].

The entropic sampling algorithm applied in conjunction with the lid method yields the LDOS previously mentioned. The first step is to identify a local energy minimum using a Monte Carlo algorithm running at constant temperature. The energy of this minimum is taken as the zero of the energy axis, and as the lower edge of the first bin in the energy histogram to be constructed. The standard entropic algorithm is modified by adding a rejection criterion: every spin configuration with an energy greater then the lid is rejected *a priori*. The lid value will therefore be the upper edge of the last bin in the energy histogram. Finally, a "bail-out" option is included: whenever a configuration of negative energy is found, a new lower energy minimum is identified and the whole process starts afresh with that new minimum used as a starting point.

III. RESULTS

Below we present results for the LDOS, $\varrho(\epsilon)$, for the EA model on square and cubic lattices of linear size $L = 30$ and $L = 8$, respectively. The energy is in all cases scaled by the number of spins N_{spin}, i.e., $\epsilon = E/N_{\text{spin}}$. The average of the lowest energy values encountered in each of the N_{sample} different runs is denoted $\epsilon_{\min}$. We consider four different valleys defined, in units of energy per spin, by the lid values $\lambda = 0.1, 0.2, 0.4$, and 0.8. The number of bins in the histogram is $N_h = 20$ for $\lambda = 0.1, 0.2$, and $N_h = 40$ and $N_h = 80$ for $\lambda = 0.4$ and $\lambda = 0.8$, respectively. We also consider for comparison the GDOS obtained by the entropic algorithm with no lid restrictions imposed. Unless otherwise specified, the sum of the density of state over all available energy bins is normalized to one.

Two types of error may affect the calculations. The first type is lack of convergence due to an insufficient number of iterations being performed. As our results show, the unrestricted entropic algorithm definitely suffers from this problem near the endpoints of the energy range. The issue is therefore the convergence of the algorithm when a lid is imposed. All results presented being averages over

$N_{\text{sample}} = 100$ different realizations of the couplings, the second error type is the statistical error on these averages.

In the entropic algorithm a large number of iterations, i.e., reaching a large n value in Eq. (3), is more important than obtaining an accurate histogram at any particular iteration as discussed in Ref. [18]. A relatively high number of iterations, $N_{\text{iter}} = 40\,000$, and a relatively low number of MC sweeps at each iteration, $N_{\text{sweep}} = 20$, is therefore chosen. The weights $h_i(E)$ of the first 50 iterations are disregarded and these iterations provide only a less naive starting guess for the density than the uniform one.

The convergence of the algorithm (with a lid imposed) is investigated using the deviation from unity of the ratio between approximations of the density of states taken m iteration steps apart, $h_n(i) = \varrho_{n+m}(i)/\varrho_n(i)$, where $1 \leqslant i \leqslant 80$ is the energy bin index, n is the iteration number, and where m is for convenience taken to be much larger than one. In Fig. 1 we show the results of calculations carried out in both 2D and 3D for a single realization of the bonds, using $m = 100$, three values of i, and $\lambda = 0.8$. The choice $\lambda = 0.8$ covers the case where good convergence is hardest to achieve as the size of the configuration space to be explored is largest. The three bin index values used show typical behavior, i.e., very similar curves are obtained for other values of i. There is, however, a caveat: since in 3D and for $\lambda = 0.8$ only a small fraction of the states lies near the lower edge of the energy spectrum, the statistical sampling is insufficient in this region (a problem easily fixed by choosing a smaller λ). The bins for the 3D case are accordingly all chosen to lie in the higher part of the energy interval. In general, our results show that after an oscillatory transient, the algorithm reaches a good convergence in the 40 000 iterations we have used throughout this work.

We now turn to the error on the LDOS averaged over many different samples. Since the sample-to-sample fluctuations of $\varrho(\epsilon)$ are rather small, the statistical errors in the graphs shown are utterly negligible. To obtain a more quantitative assessment, the error bar $\sigma(\epsilon)$ on the data presented is calculated as the standard deviation of the average LDOS, estimated over the N_{sample} independent simulations and divided by $\sqrt{N_{\text{sample}}}$. The relative statistical error is then given for each value of the energy as the ratio of $\sigma(\epsilon)/\varrho(\epsilon)$. The above procedure was carried out in both 2D and 3D, and in each case for the two lid values at the opposite ends of the range investigated, i.e., $\lambda = 0.1$ and $\lambda = 0.8$. The largest values of the relative error observed through the energy range provide relevant bounds. In 2D these bounds are 4% and 7% for $\lambda = 0.1$ and $\lambda = 0.8$, respectively. The corresponding values for the 3D system are 4% and 10%. These bounds all stem from the lowest energy bin and hence belong to the smallest value of the LDOS. Since the relative error decreases very rapidly with energy, they give a rather pessimistic view of the uncertainty of our data.

In 2D the entropic algorithm repeatedly encounters states of energy lower than the energy of the "current" lowest state, meaning that the search is repeatedly abandoned and restarted from the new lowest state. This behavior is connected to the form of the LDOS, which is, as we shall see, almost flat, except for the lowest energies. By contrast, the LDOS increases very rapidly with energy in 3D. This prevents the algorithm from fully exploring the relatively few states located at energies near the bottom of the current valley. Correspondingly, states of energy lower than the bottom of the current valley may go unnoticed and the search is restarted in only a few cases. For the same reason an unconstrained entropic algorithm is incapable of sampling a large fraction of states at the low (and high) end of the energy spectrum. By using data obtained at different lids, it is, however, possible to patch together an accurate density of states spanning approximately 40 orders of magnitude.

A. Two spatial dimensions

Our first set of results pertains to a 2D square lattice with $L = 30$. In the left panel of Fig. 2, the LDOS is plotted on a linear vertical scale versus $(\epsilon - \epsilon_{\text{min}})$ for four different lid values. The three curves corresponding to the lower lids have been vertically shifted in order to make them coincide with the fourth curve. Near the ground state, the LDOS increases

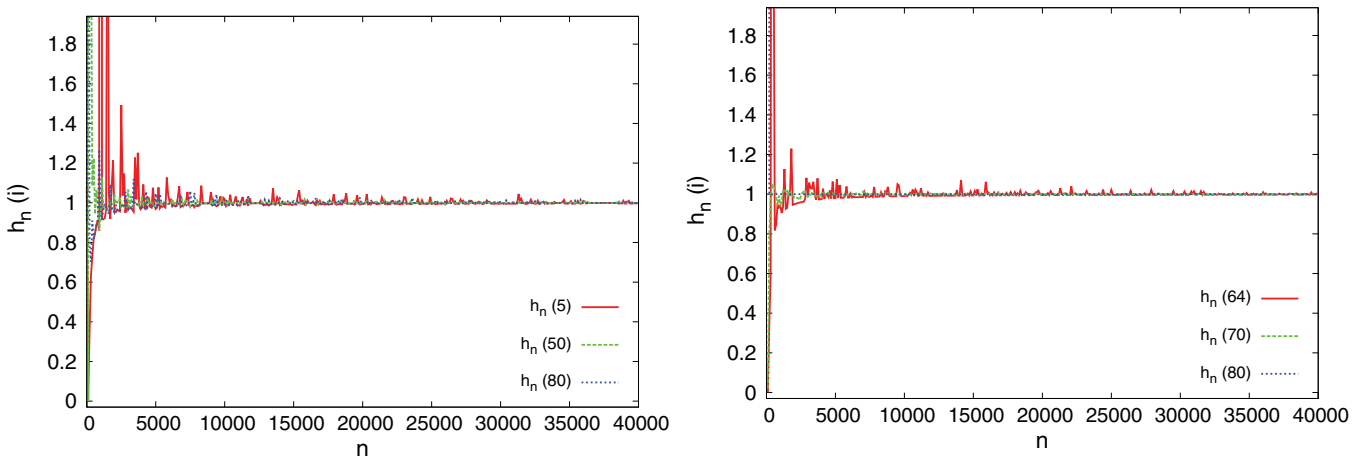

FIG. 1. (Color online) Each curve depicts the ratio of two values of the LDOS taken 100 iterations apart. The simulations are all performed at lid value 0.8. Left: A 2D system. The three curves shown correspond to values 5,50, and 80 of the energy bin index, $1 \leqslant i \leqslant 80$. Right: A 3D system. The energy bin values for the three curves are here 64,70, and 80.

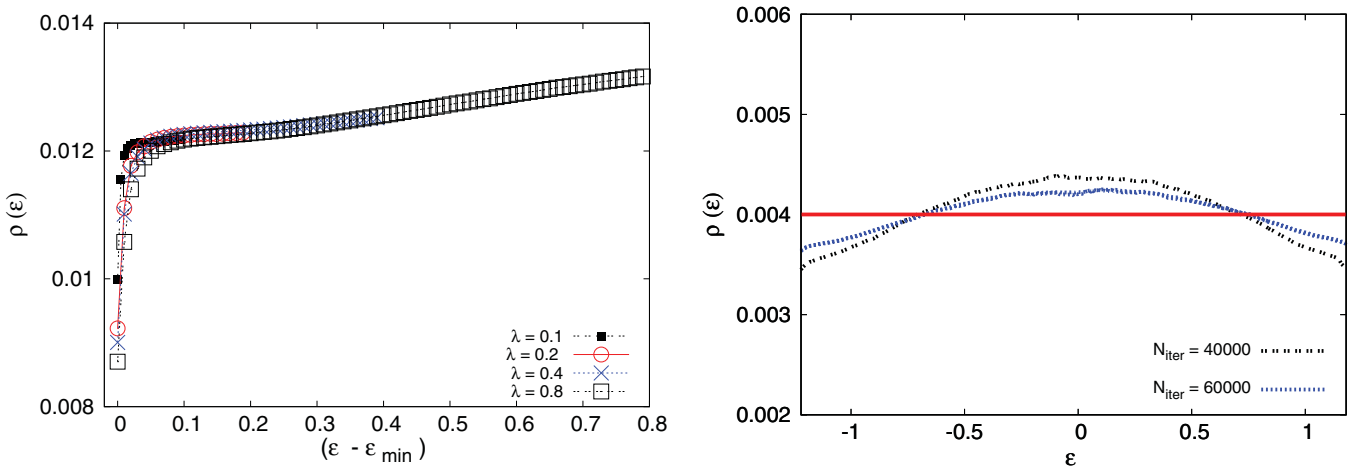

FIG. 2. (Color online) Left: LDOS for a 2D lattice with $L = 30$ for the four different lids $\lambda = 0.1, 0.2, 0.4, 0.8$. Right: The GDOS $\varrho(\epsilon)$ for two different values of the iteration number N_{iter}. All data are for a 2D lattice with $L = 30$.

very rapidly with energy. At higher energies the growth tapers off and is nearly linear in the rest of the range explored. The GDOS depicted in the right panel of the figure are obtained by running the entropic algorithm without any lid constraint. Two data sets are shown, obtained using $N_h = 250$ in both cases and a number of iterations equal to $N_{\text{iter}} = 40\,000$ and $N_{\text{iter}} = 60\,000$, respectively. For these two curves the data are averaged over ten samples. For comparison, a horizontal line is drawn as a guide to the eye. The curvature of the GDOS is seen to decrease slightly as the number of iterations increases, indicating a certain (and expected) lack of convergence of the unrestricted algorithm. Nevertheless, the relatively modest range of ϱ guarantees a passable sampling of the full range of energies available, including the region near the ground state energy of the model. As we shall see, the same situation is not achieved by the unrestricted algorithm in the 3D case.

A simplified cartoon picture of the energy landscape of the 2D EA spin glass is as follows: The landscape contains a series of valleys, all similar with respect to the internal distribution in energy of their respective configurations. Configurations belonging to different valleys have nonoverlapping energies, i.e., the lowest lying state of one valley lies above the upper rim of the valley located just below it. The valleys all have a slowly growing LDOS, and since the GDOS at a given energy mainly counts states belonging to the single valley located near that energy, the GDOS is likewise slowly growing. Note that if we disregard the initial transient, $S(E) = \ln[\varrho(E)] \propto \ln(E)$, then the average energy is simply proportional to the temperature. This excludes any thermal instability of the kind shown below to be present in 3D.

B. Three spatial dimensions

Figure 3 shows the LDOS obtained for a 3D cubic lattice with linear size $L = 8$. In the left panel, data obtained for four different lids are plotted versus $(\epsilon - \epsilon_{\text{min}})$. The right panel shows (i) the same four data sets, now horizontally shifted in order to superimpose the four lid values, together with (ii) the LDOS for the very small lid $\lambda = 0.01$, also plotted as just described. The LDOS all admit the exponential representation

$$\varrho(\epsilon) = k \exp\left(\frac{\epsilon}{\alpha(\lambda)}\right). \tag{6}$$

Their slope on a logarithmic vertical scale, $1/\alpha(\lambda)$, systematically decreases with increasing lid, starting with an almost vertical slope near ϵ_{min}. Note, however, that each straight line covers many decades of variation of the LDOS. Since the logarithm of the latter quantity is the entropy, the inverse slope α is nothing but the (microcanonical) temperature. As one would expect, the latter vanishes as the energy approaches the ground state energy, a limit enforced by $\lambda \to 0$.

The left panel of Fig. 4 shows the GDOS obtained using $N_h = 250$ and without imposing any lid constraints. The global minimum would be located on the abscissa at $\epsilon \approx -1.7$, i.e., far beyond the actual reach of the unrestricted entropic algorithm. The huge number of states present in the system simply prevents the algorithm from sampling a large fraction of the low-energy states. The line is a Gaussian fit, given by

$$\varrho(\epsilon) = k \exp\left(\frac{\epsilon}{b} - \frac{\epsilon^2}{c}\right) \quad b = 10; \quad c = 0.025; \quad k = 0.035. \tag{7}$$

The right panel shows the four different LDOS vertically rescaled to make them approximately lie on the fitted GDOS curve. These data appear as straight line segments having slope $1/\alpha(\lambda)$. The values of α for each segment are, in order of increasing lid value, $\alpha = 0.0049, 0.0058, 0.0071$, and 0.0117. A Gaussian representation of the GDOS, as in the case of the random energy model (REM) [19,20], is (by construction) inaccurate near the minimum (and maximum) of the energy range and utterly fails to reproduce the piecewise lack of curvature characterizing the LDOS at low energies.

Confirming and extending arguments previously given in Refs. [6,7,10], the exponential nature of the LDOS qualitatively explains why real 3D spin glasses lose their ability to thermally equilibrate right below the critical temperature (see Ref. [21] and references therein). The arguments given

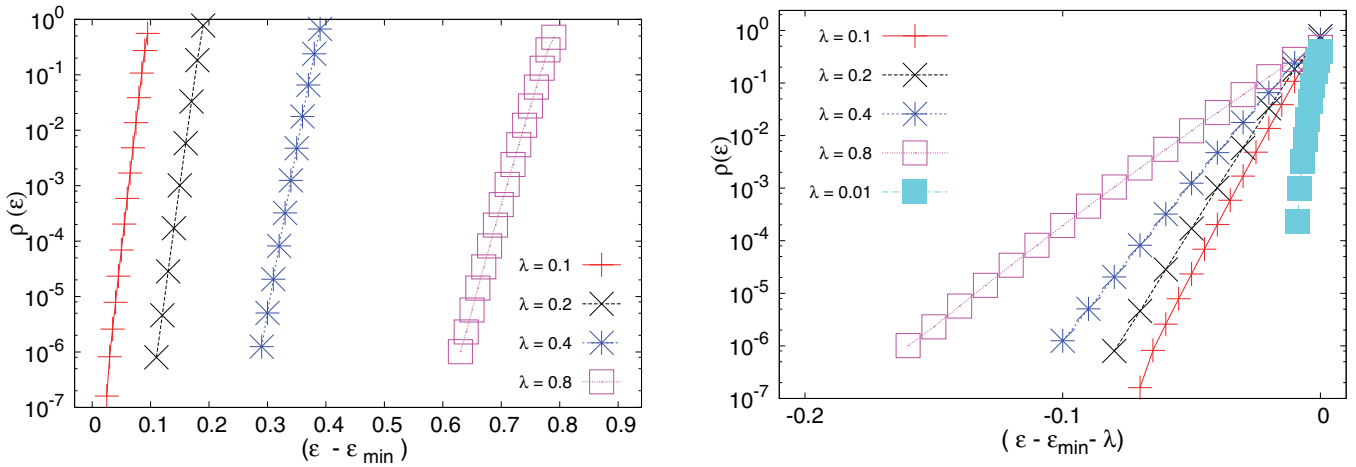

FIG. 3. (Color online) Left: $\varrho(\epsilon)$ for the four different lids $\lambda = 0.1,0.2,0.4$, and 0.8. Right: The same four quantities together with an additional LDOS obtained for $\lambda = 0.01$ are plotted on shifted horizontal scales ending in each case at the lid value. The slope of the curves is clearly seen to decrease with increasing lid value. All data pertain to a 3D lattice with $L = 8$.

below are valid in any glassy system with an exponential LDOS and link landscape topography to aging behavior, and in particular, to the origin of memory effects.

Expressed in terms of the extensive energy $E = N\epsilon$, the Boltzmann equilibrium distribution describing local equilibration in a valley is

$$P_{\text{Boltz}}(E,T) = k \exp\left(E\left[\frac{1}{\alpha(\lambda)N} - \frac{1}{T}\right]\right). \tag{8}$$

Here and in the following N denotes the number of spins which are thermally active in the valley considered, rather than the total number of spins in the system. Rescaling the α values obtained for the LDOS reflects that the energy per spin ϵ is replaced in Eq. (8) by the extensive energy variable E. For local thermal equilibrium within a valley to be possible, the sum in square brackets must have negative sign, since this guarantees that the "bottom" states of the valley have the largest probability. If the sign is instead positive, the rim states have largest probability. The valley is then abandoned with probability one and becomes irrelevant to the relaxation process.

Consider now a system locally equilibrated at $T > T_g$. Decreasing the temperature, even slightly below T_g, makes previously unaccessible valleys, namely, those with with $\alpha N < T_g$ appear. Hereby a huge number of unexplored configurations appears. These are separated by energy barriers corresponding to the internal structure of the new valleys. Effectively, a slight temperature decrease quenches the system into a local energy minimum, and thereby starts the aging process. Since the value of α slowly decreases with energy, some lower energy parts of the energy landscape remain inaccessible to the aging process for $T <\approx T_g$. If the temperature is further

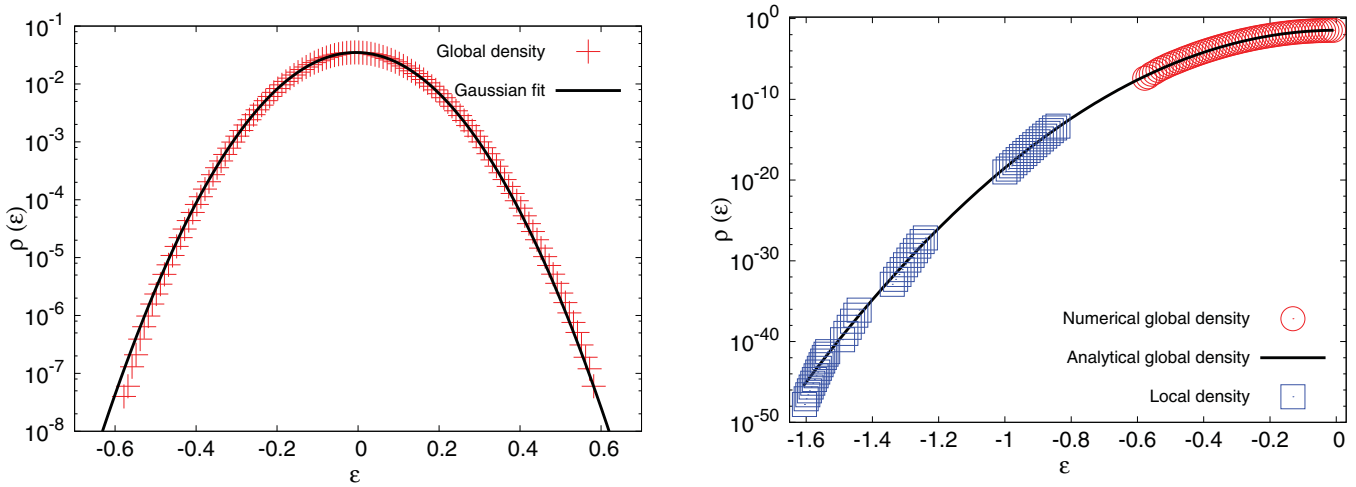

FIG. 4. (Color online) Left: GDOS (plusses) obtained by running the entropic algorithm without lid restrictions and a Gaussian fit (line). Right: The GDOS (line) obtained by extending the range of the fit shown in the left panel and the LDOS (squares) obtained for four different lids, $\lambda = 0.1,0.2,0.4,08$. The numerical GDOS (circles) appears in the rightmost corner of the figure. Note that the vertical axis spans 40 orders of magnitude. All data are for a 3D lattice with $L = 8$.

decreased, a new aging process starts in the yet-unexplored part of the landscape. Upon raising T back to its previous value, the system recovers its previous local equilibrium state (a memory effect), and the effects of aging at the lower temperature are lost (a rejuvenation effect). Rejuvenation and memory effects are well known in spin glasses and other complex systems [22–25].

Our above arguments do not suffice to identify the value of T_g. Given, however, that the latter is known for the EA spin glass, $T_g = 0.95$ [26], we can, as a consistency check, estimate the number of spins active in thermal relaxation just below T_g. Using the equilibrium average energy vs temperature curve (not shown but easily obtained using the density of states) the equilibrium energy per spin at T_g is found to be $\langle\epsilon\rangle(T_g) \approx -1.05$. This value falls between the third and fourth energy intervals in which the LDOS was numerically investigated. The average of the corresponding two α values, $\alpha \approx 0.0094$, is therefore used to estimate the logarithmic slope of the LDOS at that equilibrium energy. Using that T_g is the temperature at which the manifold of low-lying states first appears imposes $0.0094N = T_g = 0.95$. This gives $N \approx 101$ active spins, which is slightly above a fifth of the $8^3 = 512$ spins present in the system.

Let us finally consider a structural issue, i.e., the topography of the energy landscape of the 3D EA spin glass as it emerges from the present investigations. The exponential growth of the LDOS can be understood in the context of a hierarchical picture of valleys within valleys [6,7,27]. The valley rooted at the ground state contains subvalleys whose number increases exponentially with energy. Each of these has itself an exponentially growing number of internal subvalleys and so forth, down to a lower cutoff for the energy difference between top and bottom states of a valley. Since states at a given energy belong to a number of subvalleys which increases exponentially with that energy, the LDOS itself grows exponentially in energy. A glance at Fig. 4 indicates that the picture is applicable for energies per spin below ≈ -0.7. At higher energies the logarithm of the LDOS has non-negligible curvature and the picture no longer applies.

IV. DISCUSSION

Unrestricted entropic algorithms [3–5] can efficiently and for a wide range of temperatures provide thermal averages of relevant quantities in several models of physical interest. If, however, the density of state varies over, e.g., 40 orders of magnitude as is the case in the 3D EA model, low-energy states which constitute only a tiny fraction of the whole are hard to sample efficiently and accurately. Using entropic algorithms in lieu of exhaustive enumeration [6,7,10] in connection with the lid algorithm produces an accurate sampling of the energy landscape of larger systems over a wider energy range than previously possible [7,17]. As a consequence, a clear-cut difference between 2D and 3D landscape topography becomes evident and in 3D quadratic fits of the logarithm of the density of states reveal shortcomings for energies near the ground state.

In 2D the density of state has a weak, nearly linear energy dependence, except in a narrow region close to the ground state. The average energy is simply proportional to the temperature and any thermal instability is ruled out. The situation is completely different in 3D: while a parabola describes the energy dependence of the logarithm of the density of state very well over approximately 15 orders of magnitude, this Gaussian description fails near the ground state. Here the logarithm of the LDOS has instead a piecewise linear dependence on the energy. Precisely this feature explains the inability of the spin glass to equilibrate below T_g and the instability of the thermalization dynamics to small temperature changes. From a structural point of view, the form of the LDOS in 3D points to a configuration space with nested valleys and to an associated hierarchy of energy barriers, properties which are widespread in complex systems. We thus believe that the method described in this work can generally be of use in mapping out in a computationally efficient way geometrical properties of the low-energy part of the energy landscapes of complex systems.

ACKNOWLEDGMENT

P.S. would like to thank Karl Heinz Hoffmann for his hospitality and for an interesting discussion.

[1] D. J. Wales, *Energy Landscapes, With Applications to Cluster, Biomolecules, and Glasses* (Cambridge University Press, Cambridge, UK, 2003).
[2] F. H. Stillinger and T. A. Weber, Phys. Rev. A **28**, 2408 (1983).
[3] A. M. Ferrenberg and R. H. Swendsen, Phys. Rev. Lett. **61**, 2635 (1988).
[4] F. Wang and D. P. Landau, Phys. Rev. E **64**, 056101 (2001).
[5] J. Lee, Phys. Rev. **71**, 211 (1993).
[6] P. Sibani, C. Schön, P. Salamon, and J.-O. Andersson, Europhys. Lett. **22**, 479 (1993).
[7] P. Sibani and P. Schriver, Phys. Rev. B **49**, 6667 (1994).
[8] J. C. Schön and P. Sibani, Europhys. Lett. **49**, 196 (2000).
[9] J. C. Schön and P. Sibani, J. Phys. A **31**, 8165 (1998).
[10] P. Sibani, R. van der Pas, and J. C. Schön, Comput. Phys. Commun. **116**, 17 (1999).
[11] S. F. Edwards and P. W. Anderson, J. Phys. F 965 (1975).
[12] M. Picco, F. Ricci-Tersenghi, and F. Ritort, Phys. Rev. B **63**, 174412 (2001).
[13] R. N. Bhatt and A. P. Young, Phys. Rev. B **37**, 5606 (1988).
[14] H. G. Katzgraber, M. Körner, and A. P. Young, Phys. Rev. B **73**, 224432 (2006).
[15] K. H. Fischer and J. A. Hertz, *Spin Glasses* (Cambridge University Press, Cambridge, England, 1991).
[16] M. Mezard, G. Parisi, and M. Virasoro, *Spin Glass Theory and Beyond*, *World Scientific Lecture Notes in Physics*, Vol. 9. (World Scientific, Singapore, 1987).
[17] T. Klotz, S. Schubert, and K. H. Hoffmann, Eur. Phys. J. B **2**, 313 (1998).
[18] M. E. Newman and G. T. Barkema, *Monte Carlo Methods in Statistical Physics* (Oxford University Press, 1999).

[19] B. Derrida, Phys. Rev. B **24**, 2613 (1981).
[20] H. Bauke and S. Mertens, Phys. Rev. E **70**, 025102(R) (2004).
[21] G. G. Kenning, J. Bowen, P. Sibani, and G. F. Rodriguez, Phys. Rev. B **81**, 014424 (2010).
[22] K. Jonason, E. Vincent, J. Hammann, J. P. Bouchaud, and P. Nordblad, Phys. Rev. Lett. **81**, 3243 (1998).
[23] V. Dupuis, E. Vincent, J.-P. Bouchaud, J. Hammann, A. Ito, and H. Aruga Katori, Phys. Rev. B **64**, 174204 (2002).
[24] C. Josserand, A. V. Tkachenko, D. M. Mueth, and H. M. Jaeger, Phys. Rev. Lett. **85**, 3632 (2000).
[25] L. Berthier and J.-P. Bouchaud, Phys. Rev. B **66**, 054404 (2001).
[26] E. Marinari, G. Parisi, and J. J. Ruiz-Lorenzo, Phys. Rev. B **58**, 14852 (1998).
[27] P. Sibani and K. H. Hoffmann, Europhys. Lett. **16**, 423 (1991).